Receptor-oriented Pharmacophore-based *in silico* Screening of Human Catechol *O*-Methyltransferase for the Design of Antiparkinsonian Drug

Jee-Young Lee, Sunhee Baek, and Yangmee Kim*

Department of Bioscience and Biotechnology, Bio/informatics Center, IBST, Konkuk University, Seoul 143-701, Korea
**E-mail: ymkim@konkuk.ac.kr*
Received December 11, 2006

Receptor-oriented pharmacophore-based *in silico* screening is a powerful tool for rapidly screening large number of compounds for interactions with a given protein. Inhibition of the enzyme catechol-*O*-methyltransferase (COMT) offers a novel possibility for treating Parkinson's disease. Bisubstrate inhibitors of COMT containing the adenine of S-adenosylmethionine (SAM) and a catechol moiety are a new class of potent and selective inhibitor. In the present study, we used receptor-oriented pharmacophore-based *in silico* screening to examine the interactions between the active site of human COMT and bisubstrate inhibitors. We generated 20 pharmacophore maps, of which 4 maps reproduced the docking model of hCOMT and a bisubstrate inhibitor. Only one of these four, pharmacophore map I, effectively described the common features of a series of bisubstrate inhibitors. Pharmacophore map I consisted of one hydrogen bond acceptor (to Mg^{2+}), three hydrogen bond donors (to Glu199, Glu90, and Gln120), and one hydrophobic feature (an active site region surrounded by several aromatic and hydrophobic residues). This map represented the most essential pharmacophore for explaining interactions between hCOMT and a bisubstrate inhibitor. These results revealed a pharmacophore that should help in the development of new drugs for treating Parkinson's disease.

Key Words : *in silico* Screening, Methyltransferase, Bisubstrate, Parkinson's disease, Flavonoids

Introduction

The *O*-methylation of endogenous catecholamines and other catechols is catalyzed by the catechol *O*-methyltransferase[1-5] (COMT; EC 2.1.1.6.) in the presence of Mg^{+2}. COMT plays important roles in the metabolism of catecholamine, such as dopamine, a neurotransmitter. Therefore, COMT inhibitors are valuable adjunct treatments for central nervous system disorders such as Parkinson's disease and possibly schizophrenia.[6-9] Indeed, combination of COMT inhibitors and levodopa is an effective method for treating Parkinson's disease.[10-12] Also, flavonoid such as quercetin is known to be an excellent substrate for COMT

COMT exists as both a soluble form which contains 221-amino acid and a membrane-bound form with a 50-amino acid N-terminal extension. The catalytic region of COMT consists of a SAM-binding domain and an inhibitor binding domain.[13,14] Binding of Mg^{2+} to the catalytic site of COMT converts the hydroxyl groups of the catechol substrate to a more easily ionizable from and makes tight binding the catechol moiety possible. The three-dimensional structure of rat COMT (rCOMT) with bound SAM and catechol inhibitors has been determined at resolution of 2.0 Å.[15] Because human COMT (hCOMT) and rCOMT share 80% amino acid sequence identity, in a previous study we predicted the hCOMT structure using comparative homology modeling.[16-18]

Bisubstrate inhibitors, in which substrate and cofactor analogues are covalently linked, may offer opportunities for enhanced binding affinity and selectivity not available with simple substrate analogues.[19] Enzymes that catalyze chemical transformations between multiple bound substrates or a substrate and a cofactor are potential targets for bisubstrate inhibitors. For example, bisubstrate inhibitors of the insulin receptor tyrosine kinase and farnesyltransferase have been recently reported. Methyltransferases that depend on S-adenosylmethionine (SAM) are also important targets of bisubstrate inhibitors.[20,21] Bisubstrate inhibitor for COMT shows a competitive inhibition mechanism with regard to the SAM binding site and a more complex inhibition mechanism with regard to the catechol binding site.

Receptor-oriented pharmacophore-based *in silico* screening allows screening of a large number of compounds for possible interaction mode of compound into active site of receptor as well as for explaining noncovalent interactions between a protein and its ligand.[22-24] Each noncovalent contact consists of an interaction between an atom or a functional group of the target protein and an atom or functional group of its ligand. These potential interactions are used to identify ligands that are likely to bind to the known or assumed active site of a protein. To do this, the defined active site is analyzed to generate an interaction model, which consists of a list of features that a ligand must satisfy to form a reasonable interaction with the protein. These interaction models are called pharmacophores,[25,26] which are sets of interactions (chemical features or functionalities) aligned in three-dimensional space. These features, along with the excluded volume regions, based on the positions of the receptor atoms, are used to generate three-dimensional pharmacophore maps. For each library of compounds, a conformationally flexible database is constructed. This database is then searched with the set of pharmacophore maps. The resulting hits consist of various conformers of a subset of compounds that satisfy

one or more maps and, therefore, are expected to fit the active site reasonably well.

In this study, we describe receptor-oriented pharmacophore-based *in silico* screening for hCOMT using structure-based focusing (SBF) module of Cerius2.[22-25] Based on the hCOMT structure, which was generated by comparative homology modeling, we proposed a docking model for hCOMT and bisubstrate inhibitors and, furthermore, built a pharmacophore map. This map should provide useful information for the design of drugs against Parkinson's disease.

Methods

We used SBF of Cerius[2], CatDisk and CatINFO modules of Catalyst, and Homology and Discover modules of Insight II which are software packages of Accelrys, for this work. These molecular modeling were carried out on an OCTANE R12000 silicon graphics workstation.

Determination of the Three-dimensional Structure of hCOMT. In a previous study, we established a method for building the three-dimensional structure of hCOMT by comparative homology modeling. We predicted the structure of hCOMT using MODELLER[28-30] and based on the structure of the rCOMT complex with a bisubstrate inhibitor (PDB entry 1JR4). The variability in this model can be used to evaluate its reliability. Energy minimization calculations were performed with the consistent valence force field and steepest descent and conjugated gradient algorithms. Gradient on energies less than 1 kcal/mol used as convergence criteria. These calculations were performed using Discover module of Insight II. The quality of this model was analyzed by PROCHECK. The docking model for hCOMT and a bisubstrate inhibitor was proposed on the basis of the rCOMT complex structure because the sequence homology of rCOMT and hCOMT is over 80% and the active sites of the two enzymes are very similar

Receptor-oriented Pharmacophore-based *in silico* Screening. The interaction model used for this process is a list of features, such as hydrogen bonds and lipophilic interactions. These features include hydrogen bond donors (HBDs), hydrogen bond acceptors (HBAs) and lipophilicity (lipo).

Pharmacophore maps were generated with the excluded volume for the heavy atoms. The exclusion volume is the forbidden area in the active site, which defines its shape. To account for excluded volume regions occupied by the heavy atoms in the receptor, an exclusion model is generated for the active site and the surrounding receptor regions. Each atom of the receptor selected for inclusion in the model is represented as an exclusion point.

We defined the active site of hCOMT using the center and radius of the docked bisubstrate inhibitor. Next, we generated an interaction model within 10 Å of the active site center. Twenty pharmacophore maps were determined with five features for each map and the exclusion volume. The exclusion volume was built from the heavy atoms within 10 Å of the center of the active site. As a first step for verifying the 20 maps, we generated a test database using the original bisubstrate inhibitor on the docking model. We selected several maps that reproduced the docking model of hCOMT with the bound bisubstrate inhibitor. We built a second database of five known hCOMT inhibitors (Table 1) from world patent and browsed this database using selected pharmacophore maps. A three-dimensional compound library for 14 bisubstrate inhibitors are generated and searched it using the final pharmacophore maps selected from previous *in silico* screening. The ligand score (LigScore) was calculated for hits to establish a relationship between these pharmacophores and the set of inhibitors. Finally, we determined the essential pharmacophore for inhibition of hCOMT. The structures and activities of the 14 inhibitors which are collected from papers[18,19] are shown in Table 2.

Table 1. Two dimensional structure of COMT inhibitors[a]

Ligand-1	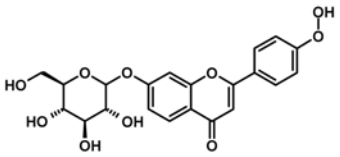
Ligand-2	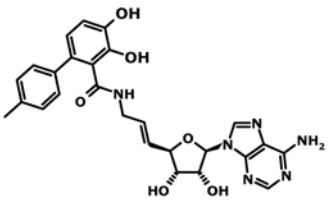
Ligand-3	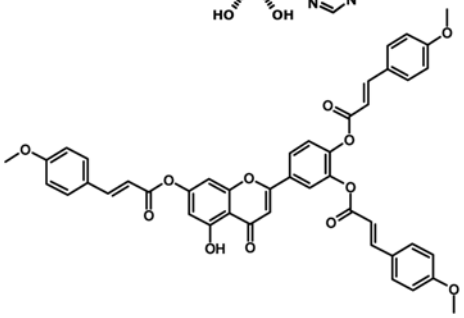
Ligand-4	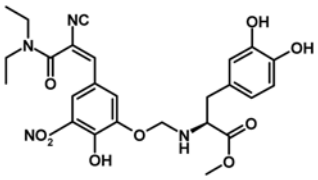
Ligand-5	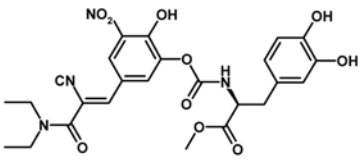

[a]Collected from world patent (http://gb.espacenet.com).

Results and Discussion

The rational design of bisubstrate inhibitors, wherein substrate and cofactor analogues are covalently linked, may provide new lead structures with enhanced binding affinity and selectivity. The concept of bisubstrate inhibitors for

Table 2. Two dimensional structure and biological activities of 14 bisubstrate inhibitors[a,b] of COMT

cmpd-1 IC_{50} = 9 nM	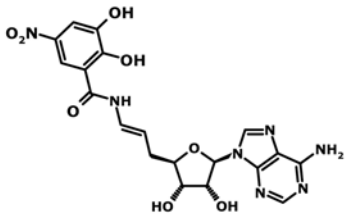	cmpd-8 IC_{50} = 90 μM	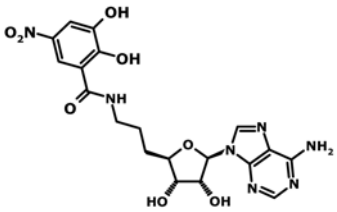
cmpd-2 IC_{50} = 23 nM	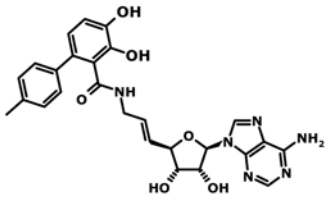	cmpd-9 IC_{50} = nd	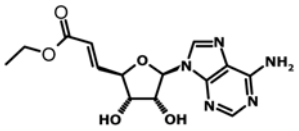
cmpd-3 IC_{50} = 21 nM	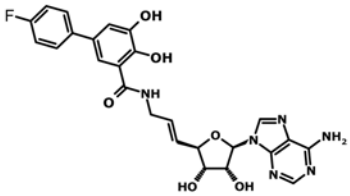	cmpd-10 IC_{50} = nd	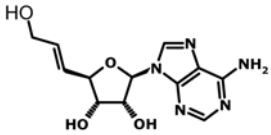
cmpd-4 IC_{50} = 23 nM	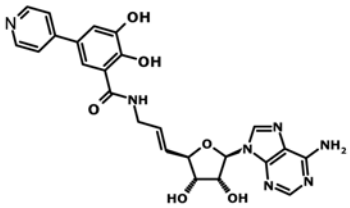	cmpd-11 IC_{50} = nd	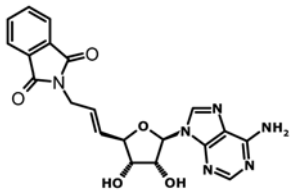
cmpd-5 IC_{50} = 27 nM	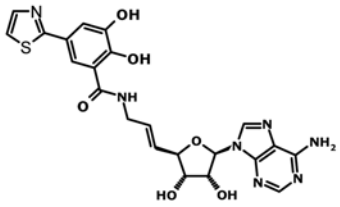	cmpd-12 IC_{50} = 213 nM	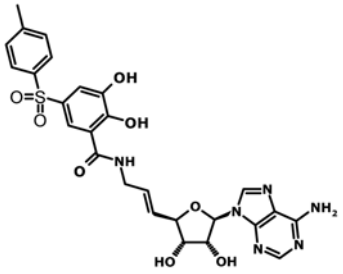
cmpd-6 IC_{50} = 97 nM		cmpd-13 IC_{50} = 608 nM	
cmpd-7 IC_{50} = 200 nM	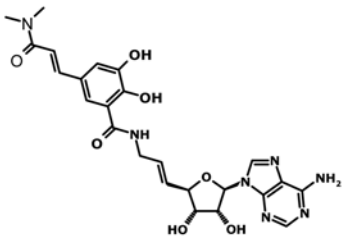	cmpd-14 IC_{50} = 1370 nM	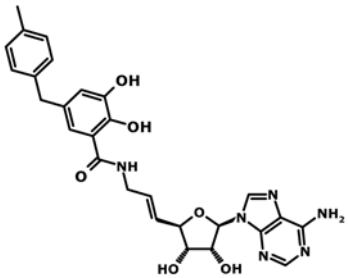

[a]Ralph, P., *et al. Chem. Bio.Chem.* 2004. [b]Christian, L., *et al. Org. Biol. Chem*. 2002. Cmpd, compound

hCOMT is illustrated in Figure 1. Bisubstrate inhibitors that block both the SAM and catechol binding sites of COMT may offer good potency and improved selectivity for hCOMT.

In our previous study, we developed a three-dimensional model of hCOMT by comparative homology modeling with rCOMT,[16,31] and, in the current study, we confirmed its validity using docking analysis. Alignment of hCOMT and rCOMT and the three-dimensional model of hCOMT is shown in Figure 2. The contacts between COMT and bisubstrate inhibitors have been identified from the X-ray crystal structure. We applied this information to the hCOMT-bisubstrate inhibitor docking model.[16] Figure 3 shows a schematic representation of the interaction model of hCOMT and the bisubstrate inhibitor as determined by Ligplot.[32]

From this docking structure, we generated a receptor-oriented interaction model for the active site of hCOMT (Figure 4). It is known that the adenine moiety of the bisubstrate inhibitor, which is important for interaction with

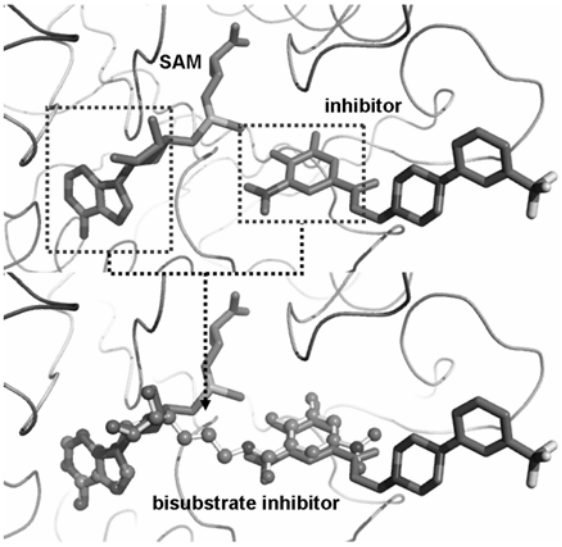

Figure 1. Concept of a bisubstrate inhibitor. Inhibitor containing the adenine moiety of SAM linked to a catechol has good potency and selectivity for hCOMT.

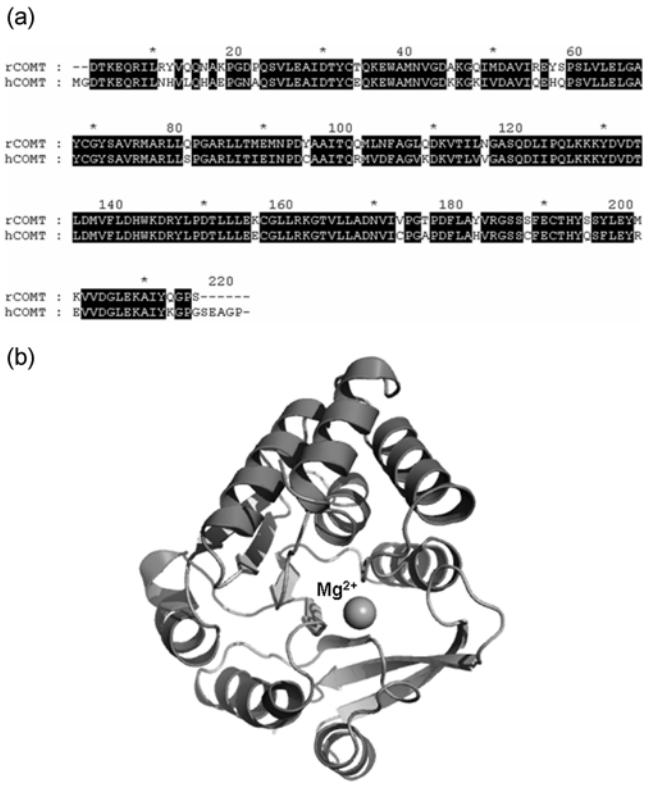

Figure 2. Result of comparative homology modeling of hCOMT. (a) Sequence alignment of hCOMT and rCOMT. The sequence identity between these two proteins is over 80%. (b) Three-dimensional structure of hCOMT.

hCOMT, has multiple hydrogen bonds with the carboxyl oxygen of Gln120, the hydroxyl group of Ser119, and a water molecule.[33] In addition, the catechol ring moiety has hydrogen bond interactions with the Mg^{2+} ion and the carboxyl oxygen of Glu199 or the side chain NH of Lys46. This model effectively describes the known interactions.

All 20 pharmacophore maps, which consisted of five

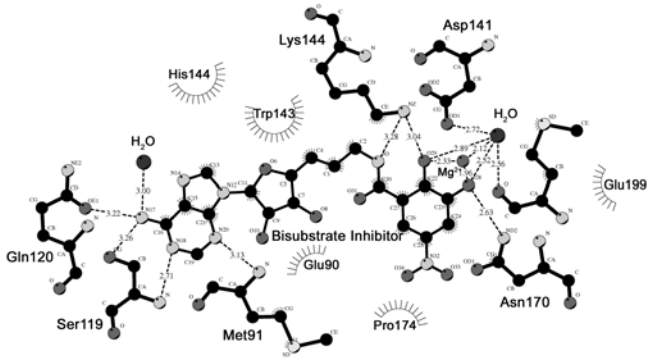

Figure 3. Schematic representation of interactions between hCOMT and the bisubstrate inhibitor using Ligplot.

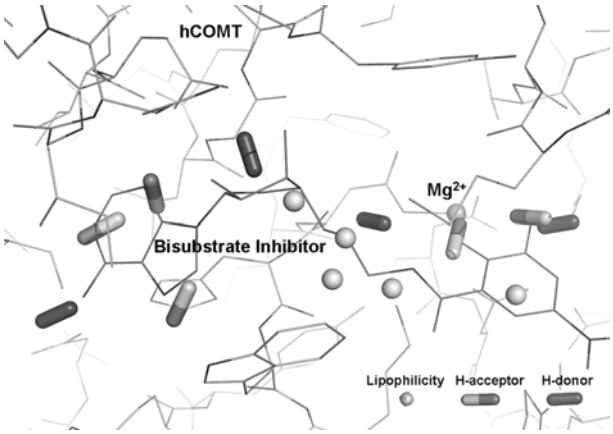

Figure 4. Interaction model of hCOMT. Receptor-oriented interaction model of hCOMT with the bisubstrate inhibitor.

Table 3. Chemical features for each of the four pharmacophore maps. Only the shadowed features differed between the maps

Pharmacophore map	Chemical features	Residue on hCOMT
Map I	HBA1	Mg^{2+}
	HBD1	Glu199
	HBD2	Glu90
	Lipo1	Trp143, Met40, Tyr66
	HBD3	Gln120
Map II	HBA1	Mg^{2+}
	HBD1	Glu199
	HBD2	Glu90
	Lipo1	Trp143, Met40, Tyr66
	HBA2-1	Asn92
Map III	HBA1	Mg^{2+}
	HBD1	Glu199
	HBD2	Glu90
	Lipo1	Trp143, Met40, Tyr66
	HBA2-2	Ser119
Map IV	HBA1	Mg^{2+}
	HBD1	Glu199
	HBD2	Glu90
	Lipo1	Trp143, Met40, Tyr66
	HBA2-3	H_2O

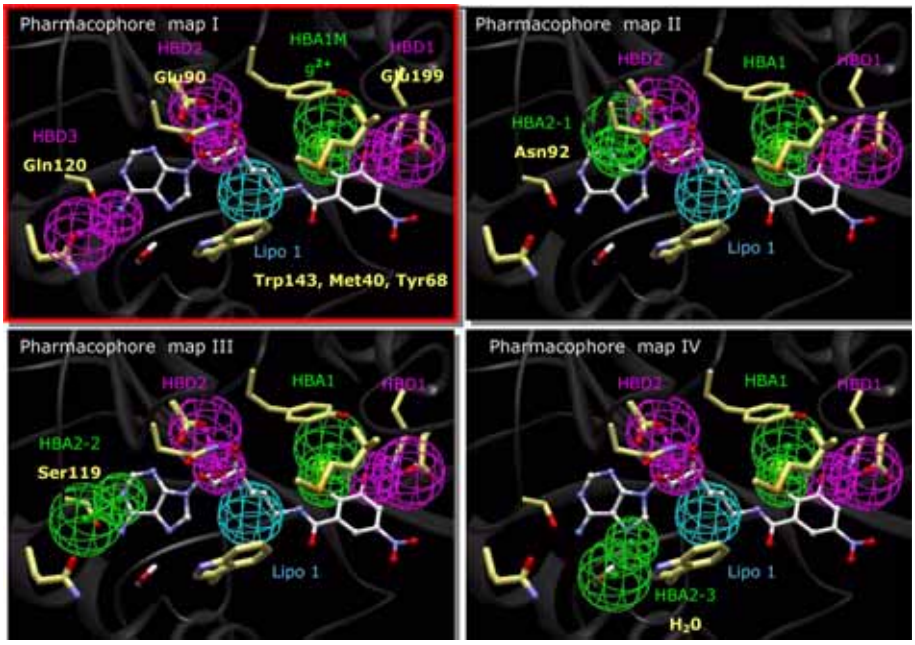

Figure 5. Pharmacophore maps for hCOMT. These maps have five chemical features for each map. One feature for each map was unique, and the other four features were shared. Only pharmacophore map I effectively represented the interactions between hCOMT and bisubstrate inhibitors.

chemical features, were randomly determined from the interaction model. To verify these maps, we used them to search the single compound database, which included only one bisubstrate inhibitor proposed by the docking model. Of the 20 maps, 4 maps reproduced the binding model of hCOMT and the bisubstrate inhibitor that was proposed in the previous step. These four pharmacophore maps (Figure 5) had four out of five features in common: HBA1 (Mg^{2+}), HBD1 (Glu199), HBD2 (Glu90), and Lipo1 (Trp143, Met40, and Tyr68); the remaining feature was different between the four maps. For example, comparison of pharmacophore maps I and IV reveals that one feature of the adenine moiety, HBA2-3, was excluded from map I, whereas the other four features were the same between the two maps. In pharmacophore map III, HBA2-2 (Ser119) was included in place of HBA2-3 in map IV. The chemical features for each of the four maps are listed in Table 4. The shadowed features in this table indicate the only differences between the maps.

Five known COMT inhibitors that were not identified by the binding or interaction models were used to generate a compound database and then searched with the four selected maps. Among these five inhibitors, two compounds, ligands 1 and 2, matched well with only pharmacophore map I (Figure 6). The mechanism by which these five inhibitors bind hCOMT was not previously known, only to discover ligand 2 was previously identified as a bisubstrate inhibitor with an IC_{50} of 23 nM. Pharmacophore map I consisted of one HBA, three HBDs, and one lipo. In map I, HBA1 was a hydrogen bond interaction with Mg^{2+}, and HBDs 1-3 were hCOMT active site residues Glu199, Glu90, and Gln120, respectively. HBD1 was involved in interaction of hCOMT with the catechol ring moiety of the inhibitor, and HBDs 2 and 3 were involved in interaction of the enzyme with the inhibitor's adenine moiety. Lipo1 was located in a region surrounded by hydrophobic residues, including Trp143, Met40, and Tyr68. This lipo site is common to all four pharmacophore maps and is well-matched with the hydrophobic region in the active site. This indicates that pharmacophore map I was the most accurate description of the interaction between hCOMT and the bisubstrate inhibitor.

To verify this conclusion, we carried out *in silico* screening for other bisubstrate inhibitors. Table 2 lists 14 bisubstrate inhibitors of COMT that we selected from the literature and that had IC_{50} values between 11 nM and 90 M. These compounds were incorporated into a three-dimensional database and searched using pharmacophore map I. The results of *in silico* screening are listed in Table 4. This analysis showed that pharmacophore map I includes features critical for the inhibition of hCOMT. Of the 14 compounds, 9 matched well with pharmacophore map I. The five most active compounds (compounds 1-5) have IC_{50} values below 27 nM and matched map I perfectly. These compounds had structures similar to the original bisubstrate inhibitor in the docking model. The remaining 4 hits had IC_{50} values above 100 nM. Compound 2 is unusual because it has a large and highly hydrophobic toluene group in the catechol ring. The catechol ring in this compound is more exposed than in other inhibitors. Therefore, the binding model of compound was slightly different than the other active compounds.

The results of the second *in silico* screening are shown in Figure 6. Although four of the nine hits (compounds 6, 7, 11, and 14) had IC_{50} values over 100 nM, they matched well with all five features of map I, and their binding models did not have obvious differences with the more active compounds. Compound 14, in particular, which was the least active (IC_{50} = 1370 nM), also hit and matched well with map I.

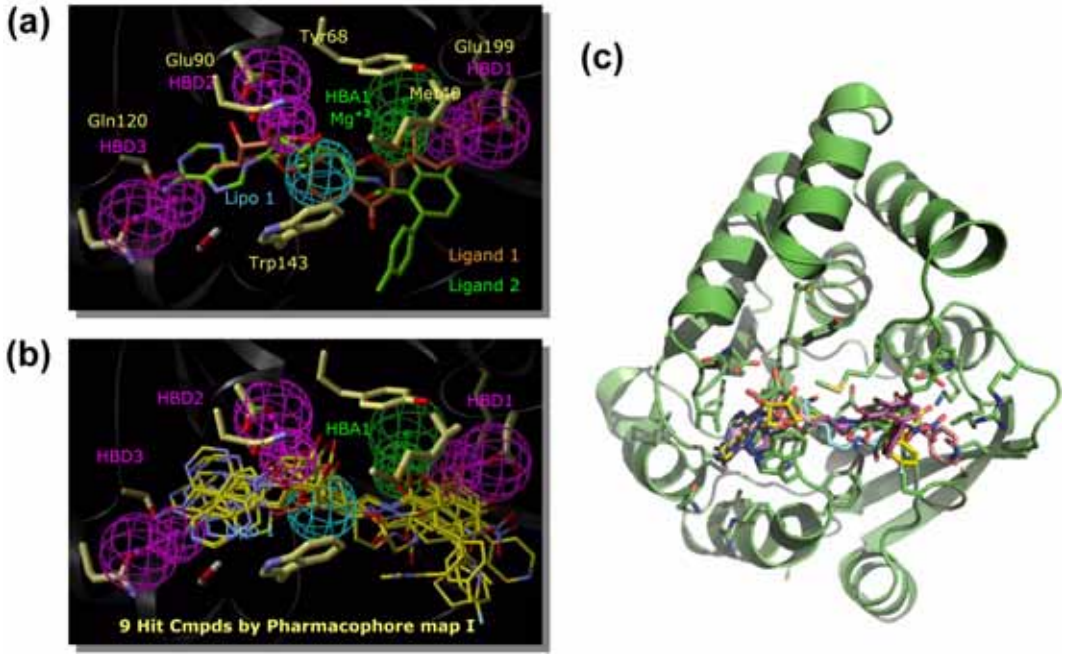

Figure 6. Results of *in silico* screening for COMT inhibitors using pharmacophore map I. (a) Only two ligands matched with pharmacophore map I. Ligand 2 in particular had a good IC_{50} value (23 nM). (b) Nine out of 14 known COMT bisubstrate inhibitors were hit using pharmacophore map I. (c) Binding model of hCOMT with hits shown in (a) and (b).

Table 4. List of nine hits for hCOMT as determined by searching of pharmacophore map I and the ligand scores calculated for these hits

Name	IC_{50} (nM)	Ligand Score (kcal/mol)
cmpd-1	11	−20.16
cmpd-4	23	−17.92
cmpd-5	27	−14.6
cmpd-3	21	−12.32
cmpd-2	23	−8.02
cmpd-6	97	−7.76
cmpd-7	200	−7.17
cmpd-14	1370	−5.09
cmpd-11	96	−2.85

Cmpd, compound

To determine the reason for these results and to refine all nine hits, we introduced a scoring function. The next step in the database search is the calculation of several scoring functions for hits to distinguish between good and poor binding configurations and to select ligands with the best binding affinities from a collection of hits. The scoring function must reliably and accurately evaluate any protein-ligand complex in a specific bound conformation. We used the ligand score provided by the SBF calculations to rank the hits. This is a fast, simple scoring function for predicting protein-ligand binding affinities,[34,35] and it is calculated based on the interaction energy between each ligand and the protein environment. Table 3 shows the ligand scores for the hits. Four out of five of the most active compounds had lower ligand scores than the four least active compounds. Because compound 2 has a toluene moiety in its catechol ring and because the active site of this group is present on the surface, its ligand score was lower than those of the other four active compounds. The ligand score of the four least active compounds were lower than those of the active compounds. As shown in Table 3, however, the ligand score for a compound is not always closely related to its biological activity. For example, compound 6 had an IC_{50} of approximately 97 nM, but its ligand score was lower than that of compound 2, which has an IC_{50} of 1370 nM. Although compound 14 matched well with map I, it had a very low ligand score, indicating that it would not bind to the active site of hCOMT.

The hits and ligand scores of various conformers of a subset of compounds that satisfy pharmacophore map I suggest that they will fit the active site reasonably well. One of the important aspects of bisubstrate inhibitor design is the length and rigidity of the linker that connects the adenine and catechol ring moieties. The lipo site of the four pharmacophore maps (Figure 5) included not only the hydrophobic region but also the linker site. Compound 8 had more flexible linker than the other compounds, which may explain why it was not hit by map I.

Therefore, in the present study, we used receptor-oriented pharmacophore-based *in silico* screening to identify the essential pharmacophore for interaction of hCOMT with a bisubstrate inhibitor. The receptor-oriented pharmacophore identified here revealed information useful for predicting the affinity of ligand binding to hCOMT. This information should be useful for the design of antiparkinsonian drugs.

Conclusion

In the present study, we developed a three-dimensional

model of hCOMT by comparative homology modeling as well as a docking model for hCOMT and bisubstrate inhibitors. We then generated a receptor-oriented pharmacophore for hCOMT and created twenty pharmacophore maps. Of these, four reproduced the proposed docking model for hCOMT and bisubstrate inhibitors. We verified these four maps by receptor-oriented pharmacophore-based *in silico* screening of a database of five known COMT inhibitors. Pharmacophore map I effectively described the interactions between hCOMT and bisubstrate inhibitors. This map consisted of five chemical features: one HBA (Mg^{2+}); three HBDs (Glu199, Gln120, and Glu90); and one lipo (Trp143, Met40, and Tyr68). A second receptor-oriented pharmacophore-based *in silico* screening was carried out for a set of 14 bisubstrate inhibitors using pharmacophore map I. Most of the five best bisubstrate inhibitors had IC_{50} values under 30 nM, were hit by map I, and were predicted to have reasonable binding to hCOMT. The low ligand scores for these compounds further supported the prediction that they bind effectively to hCOMT.

Thus, we determined the essential pharmacophore for a bisubstrate inhibitor of hCOMT and confirmed that receptor-oriented pharmacophore-based *in silico* screening is effective for determining the key interactions between proteins and their ligands. This information should help identify new drugs for treating Parkinson's disease. Our future studies will use receptor-oriented pharmacophore-based *in silico* screening and NMR spectroscopy to identify novel potent bisubstrate inhibitors of hCOMT.

Acknowledgements. This work was supported by a Molecular and Cellular BioDiscovery Research Program grant (M10301030001-05N0103-00110) from the Ministry of Science and Technology, and by Bio/Molecular Informatics Center of Konkuk University (KRF2004-F00019). Sunhee Baek is supported, in part, by the second BK21 (MOE).

References

1. Männisto, P. T.; Kaakkola, S. *Pharmacol. Rev.* **1999**, *51*, 593.
2. Zhu, B. T. *Curr. Drug. Metabol.* **2002**, *3*, 321.
3. Matsumoto, M.; Shannon, W.; Akil, B.; Lipska, K.; Hyde, T. M.; Herman, M. M.; Kleinman, J. E.; Weinberger, D. R. *Neuroscience* **2003**, *116*, 127.
4. Pekka, T. M.; Seppo, K. *Biochemistry* **1999**, *51*, 593.
5. Vincenzo, B.; Giuseppe, M. *Pharmacol. Ther.* **1999**, *81*, 1.
6. Chun-Hwi, T.; Ruey-Meei, W. *Acta Med. Okayama.* **2002**, *56*, 1.
7. Bao, T. Z. *Curr. Drug. Metab.* **2002**, *3*, 321.
8. Seppo, K. *Drugs* **2000**, *59*, 1233.
9. Dingemanse, J. *Drug Develop. Res.* **1997**, *42*, 1.
10. Jadwiga, N. *Clinical Therapeutics* **2001**, *23*, 802.
11. Daniel, O.; Hanna, P.; Ronit, G. M.; Eldad, M. *Clinical Neuropharmacology* **2001**, *24*, 27.
12. Guldberg, H. C.; Marsden, C. A. *Pharmacol. Rev.* **1975**, *27*, 135.
13. Reenila, I.; Mannisto, P. T. *Medical Hypothesis* **2001**, *57*, 628.
14. Rivett, A. J.; Francis, A.; Roth, J. A. *J. Neurochem.* **1983**, *40*, 215.
15. Maria, J. B.; Margarida, A.; Maria, L. R.; Pedro, M. M.; David, A. L.; Maria, A. C.; Patricio, S. S. *Mol. Pharmacol.* **2002**, *62*, 795.
16. Lee, J. Y.; Kim, Y. *Bull. Korean Chem. Soc.* **2005**, *26*, 1695.
17. Sánchez, R.; Šali, A. *J. of Mol. Struct.* **1997**, *398-399*, 489.
18. Kopp, J.; Schwede, T. *Pharmacogenomics* **2004**, *5*, 405.
19. Christian, L.; Birgit, M.; Armin, R.; Volker, G.; Roland, J. R.; Gerhard, Z.; Edilio, B.; François, D. *Org. Biol. Chem.* **2003**, *1*, 42.
20. Ralph, P.; Christian, L.; Roland, J. R.; Gerhard, Z.; Edilio, B.; FranAois, D. *ChemBioChem* **2004**, *5*, 1270.
21. Christian, L.; Birgit, M.; Armin, R.; Volker, G.; Roland, J. R.; Gerhard, Z.; Edilio, B.; François, D. *Angew. Chem. Int. Ed.* **2001**, *40*, 4040.
22. Paul, D. K.; Rob, B.; Scott, K.; Marvin, W.; Venkatachalam, C. M. *J. of Comp. Chem.* **2001**, *22*, 993.
23. Hoffrén, A. M.; Murray, C. M.; Hoffmann, R. D. *Curr. Pharm. Des.* **2001**, *7*, 547.
24. Luke, S. F.; Osman, F. G. J. *Braz. Chem. Soc.* **2002**, *13*, 777.
25. Pickett, S. D.; Mason, J. S.; McLay, I. M. *J. Chem. Inf. Comput. Sci.* **1996**, *36*, 1214.
26. Menana, E.; Michel, L.; Slain, C.; Fouad, C. O. *J. Mol. Model.* **2001**, *8*, 65.
27. Cosenitino, U.; Vari, M. R.; Saracino, A. A.; Pitea, D.; Moro, G.; Salmona, M. *J. Mol. Model.* **2005**, *11*, 17.
28. Martý-Renom, M. A.; Stuart, A. C.; Fiser, A.; Šanchez, R.; Melo, F.; Šali, A. *Annu. Rev. Biophys. Biomol. Struct.* **2000**, *29*, 291.
29. Šali, A.; Blundell, T. L. *J. Mol. Biol.* **1993**, *234*, 779.
30. Fiser, A.; Do, R. K.; Šali, A. *Protein Science* **2000**, *9*, 1753.
31. Šali, A. *Mol. Med. Today* **1995**, *1*, 270.
32. Wallace, A. C.; Laskowski, R. A.; Thornton, J. M. *Prot. Eng.* **1995**, *8*, 127.
33. Patricio, S. S.; Maria, A.; Vieira, C.; Antonio, P. *Pharmacology & Toxicology* **2003**, *92*, 272.
34. Krammer, A.; Kirchhoff, P. D.; Jiang, X.; Venkatachalam, C. M.; Waldman, M. *J. Mol. Graph. Model.* **2005**, *23*, 395.
35. Venkatachalam, C. M.; Jiang, X.; Oldfield, T.; Waldman, M. *J. Mol. Graph. Model.* **2003**, *21*, 289.